Acid sites on silica-supported molybdenum oxides probed by ammonia adsorption: Experiment and theory

Kazuhiko Amakawa,[1,†] Yuanqing Wang,[1,2] Jutta Kröhnert,[1] Robert Schlögl,[1,3] and Annette Trunschke[1,]*

[1]Department of Inorganic Chemistry, Fritz-Haber-Institut der Max-Planck-Gesellschaft, Faradayweg 4-6, 14195 Berlin, Germany

[2]BasCat - UniCat BASF JointLab, Technische Universität Berlin, Sekr. EW K 01, Hardenbergstraße 36, 10623 Berlin, Germany

[3]Department of Heterogeneous Reactions, Max-Planck-Institut für Chemische Energiekonversion, Stiftstraße 34-36, 45470 Mülheim a. d. Ruhr, Germany

[†]Present address: BASF SE, RCC/PO - M301, Carl-Bosch-Strasse 38, 67056 Ludwigshafen am Rhein, Germany

***Corresponding Author** Phone: +49 30 8413 4457

Fax: +49 30 8413 4401

Email: trunschke@fhi-berlin.mpg.de

Abstract

The origin of Brønsted acidity in a series of silica-supported molybdenum oxide catalysts with Mo loadings of 2.1 - 13.3 wt%, and apparent Mo surface densities of 0.2–2.5 nm^{-2}, respectively, was analyzed by ammonia adsorption investigated by temperature-programmed desorption, infrared spectroscopy, and DFT calculations. Every surface molybdenum atom in the molybdenum oxide (sub-)monolayer is involved in the interaction with ammonia, either as Lewis or as Brønsted acid site. A model is proposed that ascribes Brønsted acidity to the interaction between silanol groups and adjacent surface molybdate species under formation of pseudo-bridging Si—O(H)---$Mo(=O)_2$ species with a Mo---O(Si) distance of 2.1 Å and a N-H(OSi) distance of <1.1 Å in the formed adsorption complex of the ammonia molecule. The combined experimental and computational study contributes to an improved fundamental understanding of acidity in amorphous mixed metal oxides.

Keywords

silanol, catalyst, SBA-15, acidity, molybdenum oxide, monolayer

1. Introduction

The acid-base character of an oxide surface is an important descriptor in heterogeneous catalysis. Solid acids, such as zeolites and mixed oxides, find broad application in acid-base catalysis substituting hazardous catalysts in the homogeneous phase [1, 2], or in catalytic conversion of biomass [3, 4]. Beyond that, acidity or basicity at a solid-liquid or solid-gas interphase affect the reaction network of any catalytic reaction that involves organic reactants having an effect on C-H or C-C activation in a desired way as for example in bi-functional catalysis [5], or facilitating undesired consecutive or parallel reaction pathways with detrimental consequences in terms of the selectivity [6].

Brønsted acid-base sites at the surface of solid oxides are attributed to hydroxyl groups being potential proton donors or acceptors relative to an adsorbing or reacting molecule. Surface Lewis acid sites represent coordinative unsaturated metal ions that accept an electron pair forming a coordinate bond with an adsorbing Lewis base molecule without complete electron transfer to the metal.

The nature of acidity in crystalline silica-alumina (zeolites) has been studied extensively by experiment [7-11] and theory [12, 13] including surface science approaches that apply thin aluminosilicate films on metal single crystals as model systems [14]. It is generally accepted that bridging hydroxyl groups Al-(OH)-Si, which are located in the framework of the crystal structure, are responsible for the strong acidity of protonic zeolites. However, the origin of acid sites in amorphous SiO_2-Al_2O_3 has been strongly debated. Based on combined experimental and computational studies applying lutidine (2,6-dimethylpyridine) as probe molecule, proton transfer was attributed to the presence of pseudo-bridging silanol groups and the stabilization of silanolate species by the formation of additional O–Al and O–Si bonds [15]. Other mixed oxides

[16], such as SiO_2-MgO, SiO_2-ZrO_2, B_2O_3-Al_2O_3, B_2O_3-TiO_2, WO_3-Al_2O_3, WO_3-ZrO_2, SnO_2-SiO_2, and MoO_3-SiO_2 show acid properties as well, but the origin in particular of Brønsted acidity at the surface of such mixed oxides is less clear. In particular, basic understanding of the generation of acidity by modification of, for example, silica with another oxide and models that describe the associated proton transfer at a molecular level are essentially missing. This is also due to the diversity of binary and ternary oxides in terms of crystal structure and type of bonding (ionic versus covalent) [17], which complicates analysis in view of relations between surface structure and acid-base properties. Thus, each system requires individual examination.

Supported molybdena—silica catalysts have been applied as model systems for important catalytic reactions including selective oxidation of alcohols [18, 19], alkenes [20, 21], and alkanes [22, 23] as well as olefin metathesis [24-26]. Acidity has been identified as an important catalyst requirement responsible for formation of active carbene species in MoO_3-SiO_2 catalysts for metathesis of propene [26]. We used ammonia and propene adsorption to analyze the acidity in a series of silica-supported molybdenum oxide catalysts with Mo loadings of 2.1 - 13.3 wt%, and apparent Mo surface densities of 0.2–2.5 nm^{-2}, respectively [25]. Both, Lewis acidity attributed to coordinative unsaturated molybdenum ions as well as Brønsted acidity was found in agreement with previous reports that indicated abundant Brønsted acidity at the surface MoO_3-SiO_2 catalysts based on adsorption of probe molecules or catalytic test reactions [17, 27-32].

Molybdenum oxide [33] and silica are predominantly covalent oxides, but the coordination chemistry of Mo and Si differ significantly. The Brønsted acidity of MoO_3-SiO_2 was generally attributed to the supported molybdenum oxide itself [17], either by formation of hydroxyl groups coordinated to surface molybdate species directly (Mo-OH) [34], traces of water that lead to formation of ammonium polymolybdate species [29], or the reaction between molybdenum oxide

with the silica support that yields silicomolybdic acid [28, 30, 32]. Since the presence of Mo-OH as well as silicomolybdic acid was excluded by ^{1}H MAS- NMR and Raman spectroscopy, respectively, in the above mentioned study of a series of silica-supported molybdenum oxide catalysts [25], we initiated the present work that deals with ammonia adsorption investigated by temperature-programmed desorption, infrared spectroscopy, and DFT calculations with the aim to identify the origin of Brønsted acidity in silica-supported molybdenum oxide.

Ammonia adsorption is frequently used to probe the acidity of solid acids [8, 17, 35, 36]. The strength of Brønsted acid sites in zeolites is apparently linked to the heat of ammonia adsorption. The latter has been proposed as descriptor to quantitatively predict the rate of acid catalyzed reactions [37]. The type of acid-base interaction of ammonia with the solid surface (protonation at Brønsted acid sites *versus* coordinative adsorption at Lewis acid sites) is often probed by infrared spectroscopy [8, 17, 36]. Complete proton transfer from acidic OH groups to ammonia under formation of an ammonium ion advantageously coordinated to the negatively charged framework has been verified in zeolites [38, 39].

Based on the current investigation, a model is proposed that ascribes the Brønsted acidity in silica-supported molybdenum oxide catalysts to the interaction between silanol groups and adjacent surface molybdate species. The study was performed applying a series of catalysts that has been characterized before with respect to the structure of the surface molybdenum oxide species [40] and catalytic properties in oxidation of propane [40] and propene metathesis [25].

2. Experimental and theory

2.1 Preparation and characterization of silica-supported molybdena

Molybdenum was introduced on the surface of mesoporous silica SBA-15 using an anion exchange procedure via amino-functionalized SBA-15 as an intermediate followed by a final calcination, yielding MoO_x/SBA-15 catalysts containing highly dispersed surface molybdena species while preserving the cylindrical mesopore structure of SBA-15. Details of preparation and structural characterization are reported elsewhere [25, 40]. Table 1 summarizes Mo loading, surface density of molybdenum and silanol groups, and specific surface area A_s.

Table 1. Properties of MoO_x/SBA-15[a]

Specimen	Mo loading (wt%)	Surface density		A_s (m^2/g)
		Mo (nm^{-2})	SiOH (nm^{-2})	
SBA-15	0	0	1.6	859
2.1Mo	2.1	0.21	1.1	637
5.1Mo	5.1	0.58	0.88	554
6.6Mo	6.6	0.85	0.68	490
8.2Mo	8.2	1.1	0.51	457
13.3Mo	13.3	2.5	0.07	332

[a] See reference [40] for details of estimation methods.

2.2 Ammonia adsorption

2.2.1 Fourier Transform infrared spectroscopy (FTIRS)

The FTIR experiments were carried out in transmission mode using a Perkin Elmer 100 FTIR spectrometer equipped with a DTGS detector at a spectral resolution of 4 cm^{-1} and accumulation of 64 scans. The samples were pressed (125 MPa) into self-supporting wafers, which were placed in an in-situ IR cell. The IR cell was directly connected to a vacuum system (residual pressure of $3 \cdot 10^{-6}$ Pa) equipped with a gas dosing line. Ammonia was dosed at 353 K at the

pressure up to 7 hPa. In each experiment, the spectrum taken before probe dosing was used as background. Contribution of gas phase species was corrected by subtracting the spectrum without sample wafer. The spectra were normalized with respect to the areal weight density of the wafer. The concentration of ammonia adsorption sites were estimated using the band at 1614 and ~1430 cm^{-1} for Lewis acid sites and Brønsted acid sites, respectively. Extinction coefficients of 16 cm μmol^{-1} (Brønsted acid sites) and 1.46 cm μmol^{-1} (Lewis acid sites) were used [41].

2.2.2 Temperature-Programmed desorption of ammonia (NH_3-TPD)

Temperature-programmed desorption of ammonia (NH_3-TPD) was performed using a fixed bed reactor. About 30 mg of catalyst was used. Adsorption of NH_3 was done at 353 K by feeding 1% NH_3 in Ar (40 ml/min) for 0.5 h. After flushing the reactor with He at 353 K for 0.5 h, the bed temperature was raised with a heating rate of 10 K/min in He flow (40 ml/min). Desorption of NH_3 was monitored by a quadrupole mass spectrometer (OmniStar GSD301, Pfeiffer) using the signal of m/e = 16. The helium signal (m/e = 4) was used as internal standard.

2.3 Theory

Density functional theory (DFT) calculations were performed to simulate Lewis and Brønsted acidity of the silica-supported molybdenum oxides by applying cluster models adapted from previous studies [42-46]. The Becke three-parameter hybrid functional with Lee–Yang–Parr correlation functional (B3LYP) together with Ahlrichs' triple-zeta split-valence basis set augmented by polarization functions (def2TZVP or def2TZVPP, respectively) were chosen for the calculations [47, 48]. Grimme's dispersion correction and ultrafine integration grids for numerical integrations were adopted [49]. Each optimized structure (see structures in Figures 9 and 10) was subsequently analyzed in terms of harmonic vibration frequencies at the same level

and characterized as a minimum (no imaginary frequency) or a transition state (one imaginary frequency). In frequency calculations, a scaling factor of 0.9783 was used derived from normalizing the experimentally observed asymmetric bending vibration (1635 cm^{-1}) to that from the free NH_3 molecule (1671.27 cm^{-1}) calculated at the B3LYP/def2TZVP level. All calculations were performed using Gaussian 09 packages [50]. The images were generated using the pragram GaussView 6.

3. Results and discussions

3.1 Structure of MoO_x/SBA-15

The structural characterization of the present series of MoO_x/SBA-15 catalysts by N_2 physisorption, XRF, XRD, SEM-EDX, IR, Raman, UV-vis, O K-edge NEXAFS, and Mo K-edge XANES/EXAFS has been reported elsewhere [40]. Main findings relevant for the present investigation are summarized briefly in the following. Irrespective of the molybdenum loading, two-fold anchored tetrahedral di-oxo $(Si\text{-}O\text{-})_2Mo(=O)_2$ structures are formed at the expense of surface silanol groups at the surface of silica SBA-15. A fraction of surface silanol groups undergoes hydrogen bonding with the molybdena species (Fig. 1).

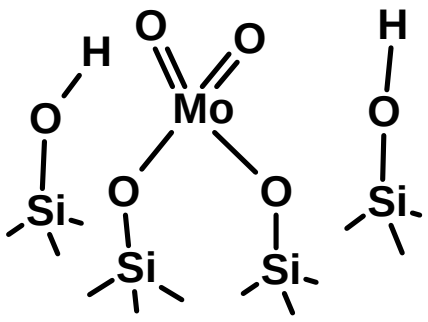

Fig. 1. Schematic illustration of the proposed predominant structure of molybdenum oxide species at the surface of mesostructured silica SBA-15 after dehydration.

Probing hydroxyl groups by FTIR spectroscopy (Fig. 2A) reveals that the introduction of molybdenum leads to the progressive consumption of isolated silanol groups characterized by the band at 3745 cm^{-1} and the occurrence of hydrogen-bonded hydroxyl groups indicated by the broad IR band at ~3600 cm^{-1}. The electronic structure around the molybdenum atoms probed by UV-vis spectroscopy remains similar with increasing Mo loading, suggesting a modest structural variation of molybdena species upon the variation in the coverage of silica [40]. The characteristic doublet of Raman bands at 970~1000 cm^{-1} (Fig. 2B) due to ν(Mo═O) of dispersed surface molybdena species [51] becomes broader and red-shifted at low metal loadings, which indicates hydrogen-bonding interactions between the surface molybdena species and neighboring silanol groups [40]. At the highest Mo loading, intense Raman bands due to crystalline MoO_3 (*e.g.*, 993 and 817 cm^{-1}) [52] were observed although this component represents only ~3% of total Mo atoms in the material (thus almost invisible in UV-vis) [40], which is due to the very high Raman scattering cross section of MoO_3 [53, 54]. No peak related to Keggin-type silicomolybdic acid ($H_4SiMo_{12}O_{40}$) at 240 cm^{-1} [30] was detected in the Raman analysis (Fig. S1). Overall, no indication for the presence of hydroxyl groups other than silanol (e.g. Mo—OH, or silicomolybdic acid $H_4SiMo_{12}O_{40}$) was obtained by the structural analysis [25], which is in agreement with a previous *in-situ* Raman study using isotope labeling technique [55]**.**

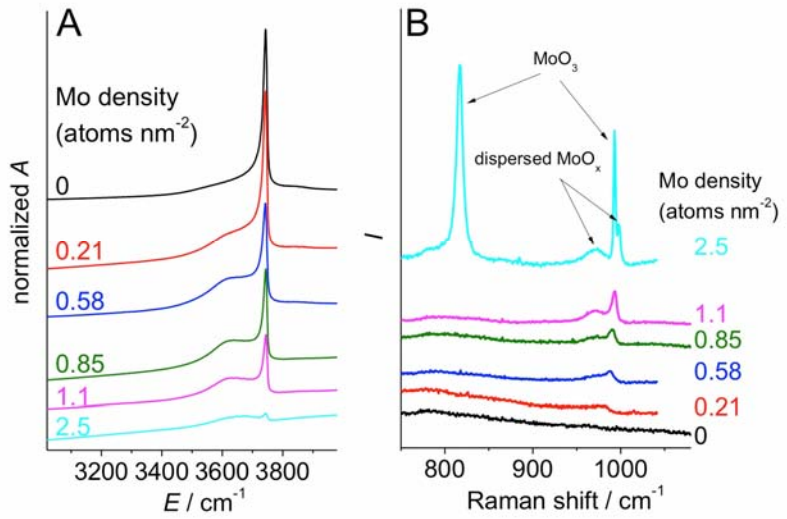

Fig. 2. (A) FTIR, and (B) Raman (excitation at 1.96 eV (632 nm)) spectra of dehydrated MoO_x/SBA-15 measured at room temperature. The samples were pretreated in 20% O_2 in Ar at 823 K for 0.5 h.

3.2 Ammonia adsorption experiments

3.2.1 NH_3-TPD

The NH_3-TPD profiles (Fig. 3A) show adsorption of ammonia at all MoO_x/SiO_2 catalysts. With increasing Mo loading the amount increases. Bare SBA-15 does not adsorb ammonia (Fig. 3A; black line). The density of desorbed ammonia molecules exhibits a linear correlation with the nominal surface Mo density, yielding an areal density of 0.22 NH_3 molecules per molybdenum atom (Fig. 3B). This observation suggests a relationship between the adsorption sites of ammonia molecules and occurrence of molybdenum oxide surface species.

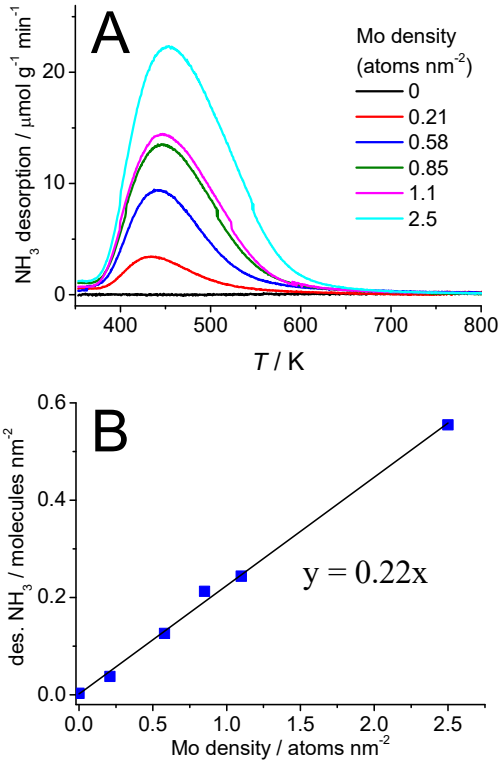

Fig. 3. Profiles of temperature-programmed desorption of ammonia (NH_3-TPD) from MoO_x/SBA-15 at a heating rate of 10 K min^{-1} (A), and correlation between the surface Mo density and the amount of desorbed ammonia (B). The samples were pretreated in 20% O_2 in Ar at 823 K for 0.5 h followed by ammonia adsorption at 353 K by feeding 1% NH_3 in Ar, and subsequent purge in a He stream at 353 K for 0.5h.

The NH_3-TPD profiles are characterized by a broad single peak centered at ca. 450 K, which indicates relative weak acidity. The slight upward shift of the peak temperature is probably due to a kinetic artifact of the measurement due to the re-adsorption of desorbed ammonia [56]. Notably, inhomogeneity of the adsorption sites with respect to the desorption energy is indicated by the peak shape characterized by a greater tailing on the high-temperature side than the low-temperature side, because a uniform strength of acid sites should give an asymmetric desorption profile with an extended tailing structure at the low-temperature side [56].

3.2.2 Infrared spectroscopy

Ammonia is very frequently used as probe molecule to characterize surface acidity of oxides by infrared spectroscopy. Due to its small size (3.70 Å x 3.99 Å x 3.11 Å) [57], the molecule captures quantitatively acid sites even in micropores. According to the Pearson HSAB principle, NH_3 is classified as hard base. Consequently, it strongly interacts with hard acids, such as small or highly charged metal cations and protons of hydroxyl groups. A band at 1600-1630 cm^{-1} arises from the asymmetric bending vibration ν_4(as) of coordinatively bound ammonia molecules, which gives notice of Lewis acidity [8, 17, 36]. Formation of the corresponding protonated species (ammonium ions) is indicative of Brønsted acidity relative to NH_3, and displayed by the asymmetric deformation vibration ν_4(as) of adsorbed ammonium ions at 1390-1490 cm^{-1} [8, 17, 36].

Fig. 4 shows the IR spectra of adsorbed ammonia on MoO_x/SBA-15 (0.58 Mo nm^{-2}) at different ammonia pressure up to 7 hPa. Continuous accumulation of adsorbed ammonia both on Lewis acid sites as NH_3 and on Brønsted acid sites as NH_4^+ is evidenced by the characteristic vibrations at 1614 cm^{-1} (Lewis sites) and 1435 cm^{-1} (Brønsted sites) observed in the entire range of the ammonia dosing pressure. All the other MoO_x/SBA-15 materials with different surface Mo density showed similar increase of ammonia adsorbed on both Lewis and Brønsted acid sites upon increasing the ammonia pressure (spectra not shown). In contrast, bare SBA-15 showed only physisorbed ammonia [36, 58] characterized by a band at 1635 cm^{-1} (Fig. S2), suggesting the absence of acid sites, which is in agreement with the NH_3-TPD result (Fig. 3).

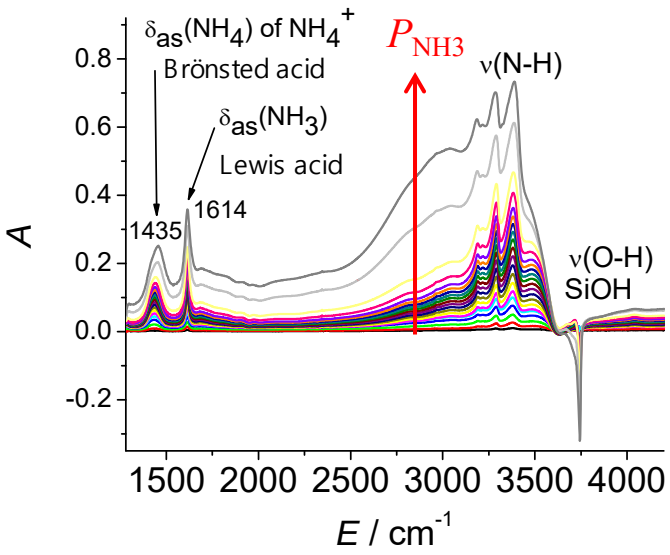

Fig. 4. IR spectra recorded after ammonia adsorption on MoO_x/SBA-15 (0.58 Mo nm^{-2}) at 353 K. Ammonia pressure was increased stepwise up to 7 hPa; The samples were pretreated in O_2 at 823 K and at 20 kPa for 0.5 h; The spectrum recorded before dosing ammonia was used as reference.

The spectra shown in Fig. 4 are differences between absorbances of the samples after and before adsorption of NH_3. Therefore, negative absorption indicates the extinction of hydroxyl groups either by consumption due to protonation of ammonia or due to occurrence of hydrogen bonding between isolated silanol groups at 3745 cm^{-1} and adsorbed ammonia that leads to the occurrence of broad components at around 3000~3600 cm^{-1}, which overlap with N-H stretching vibrations.

Evacuation for 1 h after ammonia adsorption at the maximum equilibrium pressure (7 hPa) leaves certain density of ammonia held on both Lewis and Brønsted acid sites on the surface except bare SBA-15 (Fig. 5A). Increasing the Mo density leads to an increase of the band intensities but does not change the band positions (Fig. 5A), suggesting a similar nature of acid sites, which is in accordance with the NH_3-TPD results (Fig. 3). It is noted that prolonged

evacuation for 16 hours reduced the intensity of adsorbed ammonia (data not shown), indicating that desorption can be driven by an entropic term (*i.e.* pressure of ammonia in the gas phase), implying a low activation barrier, which in turn indicates a weak acid strength.

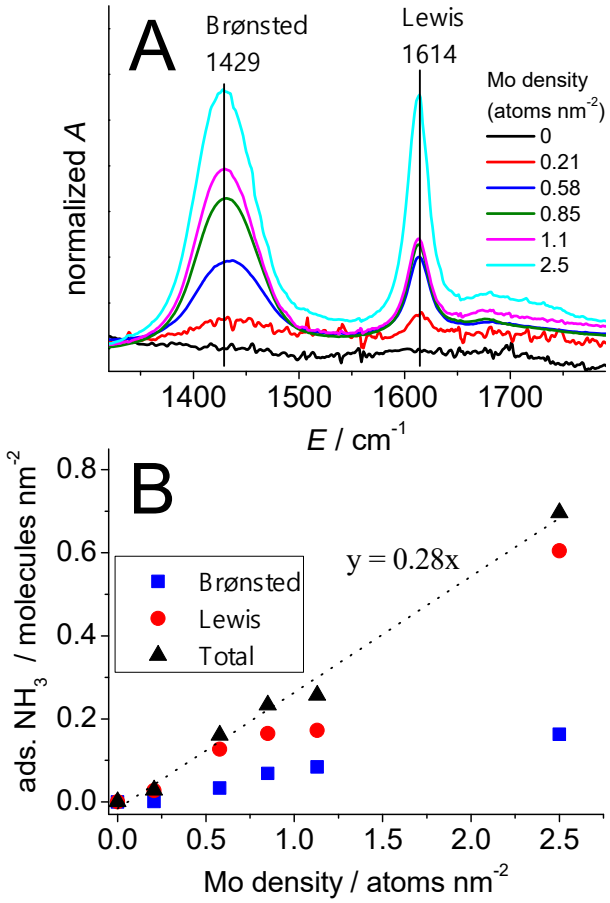

Fig. 5. Quantification of adsorbed ammonia on MoO_x/SBA-15 after evacuation: (A) IR spectra recorded after ammonia dosing (7 hPa, 353 K) and subsequent evacuation for 1h; (B) Estimated concentration of ammonia adsorption sites using the bands at 1614 and ~1430 cm^{-1} for Lewis acid sites and Brønsted acid sites, respectively. The catalysts were pretreated in O_2 at 823 K and at 20 kPa for 0.5 h.

At the state after 1 h of evacuation, the density of Lewis and Brønsted acid sites was estimated using the IR peak area applying reported extinction coefficients [41] (Fig. 5B). A quasi-linear increase was observed both for Lewis and Brønsted acid sites, yielding an areal

density of total acid sites of 0.28 NH_3 molecules per Mo atom. The comparison to the quantification by NH_3-TPD (Fig. 3) results in a good linear correlation (Fig. 6). The slope in Fig. 6 is slightly higher than unity, which is likely due to the following reasons: (1) difference in the amount of retained ammonia upon the removal of ammonia in the gas-phase (*i.e.*, He stream at atmospheric pressure for 0.5 h in the NH_3-TPD experiments, evacuation for 1 h in the IR experiments), (2) inhomogeneous thickness of the sample wafer used in the IR experiments, (3) temperature gradient within the samples, (4) artifacts in the integration of IR band area (e.g. baseline definition), and (5) difference in extinction coefficient. Nevertheless, as a first approximation, quantification using the two different techniques provides good agreement.

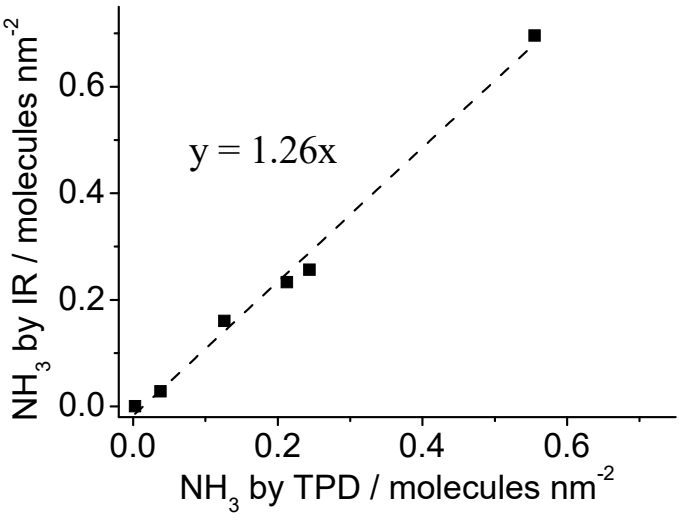

Fig. 6. Quantification of adsorbed ammonia on MoO_x/SBA-15 at 353 K by NH_3-TPD (abscissa) and IR (ordinate) showing a linear correlation; In NH_3-TPD, ammonia was adsorbed by feeding 1% NH_3 in Ar followed by purging with He at 353 K for 0.5h. IR data were measured after dosing 7 hPa of ammonia and subsequent evacuation for 1 h; See also Figs. 3 and 5 for the original data.

Integrating the intensity of the bands at 1435 and 1614 cm^{-1} with increasing equilibrium pressure (see for example Fig. 4), the amount of adsorbed ammonia at different ammonia

pressures was derived (Fig. 7). Adsorption on both Lewis and Brønsted acid sites shows Langmuir-type pressure dependence (Figs. 7A and B), suggesting a monolayer-type adsorption. Fitting to the Langmuir equation [59] results in a good, but certainly imperfect agreement with the experimental results (solid lines in Figs. 7A and B), suggesting inhomogeneity of the adsorption sites, which is in agreement with the implication from analysis of the NH_3-TPD profiles. The fraction of Brønsted acid sites among the total acid sites (Fig. 7C) remains in a range of 0.13~0.17 in the entire ammonia pressure range, suggesting that both sites exhibit a similar adsorption energy.

Similar Langmuir-type adsorption isotherms were obtained for all MoO_x/SBA-15 catalysts (data not shown). Fig. 8A summarizes ammonia uptake at the monolayer adsorption capacity (coverage θ=1), exhibiting again (compare with Fig. 5B) a quasi-linear correlation to surface Mo density. Significantly, the densities of total (*i.e.,* Lewis and Brønsted) acid sites follows approximately one-to-one correlation to the surface Mo density (Fig. 8A), indicating that nearly every molybdenum atom acts as either a Lewis or a Brønsted acid site. The fraction of Brønsted acid sites estimated at θ=1 ranged between 0.11~0.22, where a maximum was observed at Mo density of 1.1 atoms per square nanometer (Fig. 8B).

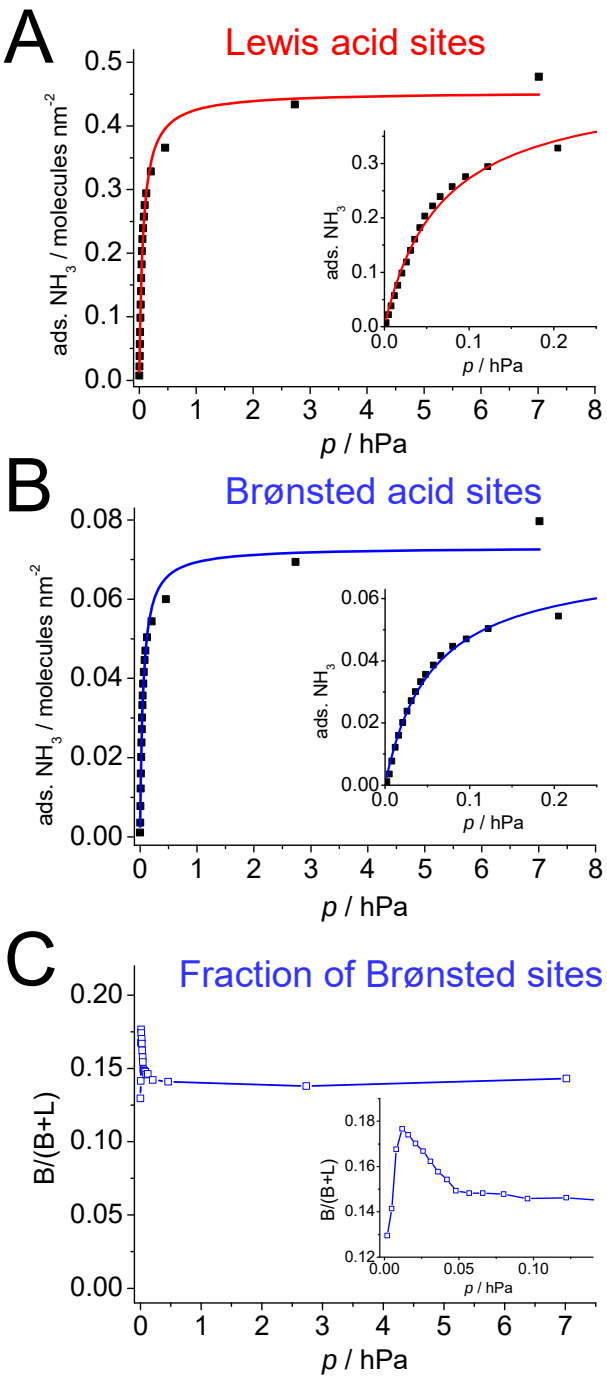

Fig. 7. Adsorption isotherms of ammonia on MoO_x/SBA-15 (0.58 Mo nm^{-2}) at 353 K plotted using the IR bands of Lewis (A) and Brønsted (B) acid sites, and the fraction of Brønsted sites (C); The lines in (A) and (B) fit to the Langmuir equation; The insets in (A) and (B) show magnification at low pressures; See Fig. 4 for the corresponding raw spectra.

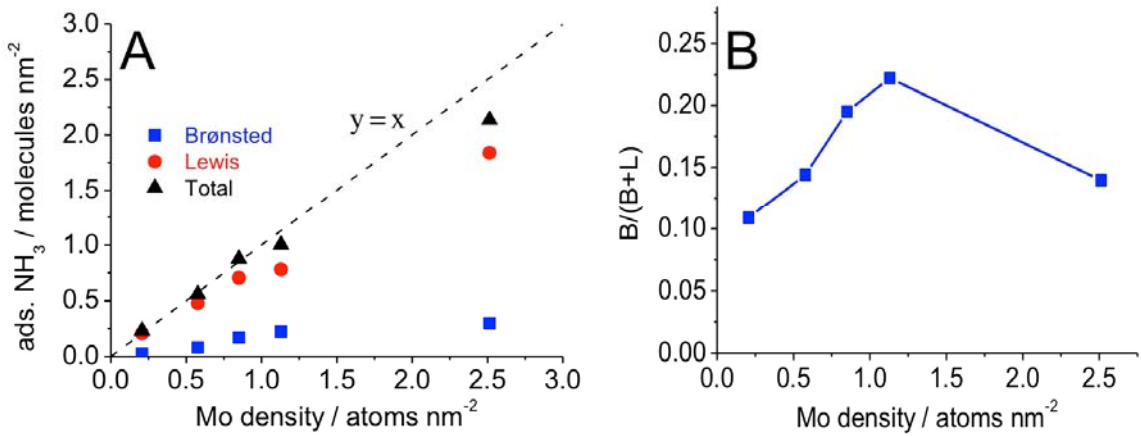

Fig. 8. Density of adsorbed ammonia on MoO_x/SBA-15 at θ=1 and T = 353 K as a function of nominal surface Mo density (A); The densities of Lewis and Brønsted acid sites were estimated using the IR bands at 1614 and ~1430 cm^{-1}, respectively (Fig. 5A); Fraction of Brønsted acid sites in relation to all acid sites (i.e. Brønsted plus Lewis) estimated by ammonia adsorption on MoO_x/SBA-15 at θ=1 and T = 353 K as a function of Mo surface density (B).

In summary, bare SBA-15 shows no significant adsorption of ammonia (Figs. 3 and 5), but deposition of molybdenum oxide introduces Bønsted acidity. The experimental results suggest that virtually every molybdenum atoms creates an acid site either in Lewis or Brønsted form. It is reasonable to assume that coordinative unsaturated metal centers are capable to accept the lone pair of the Lewis base ammonia. In the present case, the Mo(VI) centers in the predominant di-oxo $(Si\text{-}O\text{-})_2Mo(=O)_2$ structure in coordinative unsaturated tetrahedral geometry (Fig. 1A) most probably host ammonia molecules to form Lewis acid-base pairs. The diagnosing vibration band for ammonia coordinating to Lewis acid sites is sharp and remains at 1614 cm^{-1} irrespective of the Mo loading (Fig. 5A), which suggests a similar nature of Lewis acid sites in the entire Mo loading range. Hxdroxyl groups at Brønsted acid sites capable of protonating ammonia represent approximately 10~20 % of total Mo atoms (Figs. 7 and 8B). Given no indication for the presence of possible sources of protons other than silanol groups (*e.g.,* Mo-OH, or silicomolybdic acid $H_4SiMo_{12}O_{40}$), silanol groups are only possible candidates for the

considerable amount of Brønsted acid sites. The coverage of acid sites by ammonia depends on the adsorption condition applied. In the present case of MoO_x/SBA-15, only about 20~30 % of coverage remains after removal of ammonia by evacuation at 353 K (compare Figs. 5 and 8). In ammonia adsorption experiments in catalysis research for quantification of acid sites, it is often assumed that a full coverage is sustained after ammonia dosing followed by removal of gas-phase ammonia [60, 61]. However, the present study shows that this general assumption is not always valid when the adsorption is stronger than physical adsorption (Fig. S2), but weak enough to allow partial desorption upon removal of the gas phase.

3.2.3 Theory

In order to explore the local strucutres that might be responsible for Lewis and Brønsted acidity in MoO_x/SBA-15, DFT calculations emplyoing a series of cluster models were performed. As shown in Fig. 9 A, supported Mo oxide species are represented by a tetrahedral di-oxo (Si—O—)$_2$Mo(=O)$_2$ unit anchored on top of a silsesquioxane cluster ($Si_8O_{12}H_8$), which has been used to represents the SBA-15 support in previous studies [42-44, 46]. To simulate the Lewis acidity, an ammonia molecule was located in the vicinity of the molybdenum atom in the molybdenum dioxo species as an initial guess for geometry optimization. In the optimized structure (Fig. 9A), the ammonia molecule is coordinated to the Mo atom forming a trigonal bipyramidal geometry. Examination of the differences in electron density that occur upon ammonia adsorption clearly shows that electron density decreases at the N atom and increases in the region between the N and Mo atoms, which is indicative of a donative bond according to a Lewis base-acid interaction (Fig. S3). The adsorption energy of ammonia, as defined in Eq.1,

$$E_{ads} = E_{NH_3+Mo/SBA-15} - (E_{NH_3} + E_{Mo/SBA-15}) \quad (1)$$

where E_{NH_3} and $E_{Mo/SBA-15}$ are the total electronic energies of the free ammonia molecule and supported molybdenum oxide species system, respectively, and $E_{NH_3+Mo/SBA-15}$ is the total electronic energy of the geometrically optimized interaction complex (Fig. 9A), was calculated to be -19.8 kcal/mol. The value is higher compared to the experimentally determined heat of adsorption of ammonia on molybdenum oxide [62], suggesting a specific interaction between supported molybdenum oxide species and silica, but lower compared to calculated adsorption energies in amorphous [63], and crystalline [64] silica-alumina, which is in agreement with the stronger acid sites experimentally observed by temperature-programmed desorption of ammonia on silica-alumina [64, 65]. In addition, the calculated asymmetric bending vibration of coordinated ammonia is 1617 cm^{-1} (scaled), which is comparable to the experimental value of 1614 cm^{-1}. These results support that the coordinative unsaturated molybdenum atoms in the tetrahedral di-oxo structure can provide Lewis acidity.

The Brønsted acidity of silanol groups was at first investigated for bare SBA-15. An ammonia molecule was approached to the silanol group located on top of the silsesquioxane cluster (Fig. S4) and the N-H distance was reduced stepwise to form an ammonium ion. The relaxed potential energy scan (PES) curve shows that with decreasing N-H distance the electronic energy increases monotonically as well as the O-H distance in the silanol group, indicating that the deprotonation of the silanol group by ammonia in the present model is thermodynamically unfavorable. The result confirms the experimental finding that bare SBA-15 does not show Brønsted acidity with respect to ammonia.

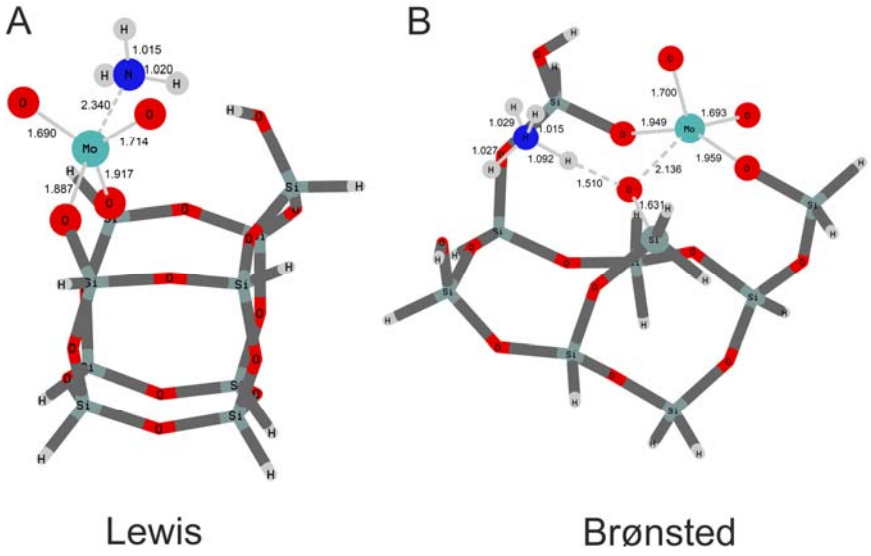

Fig. 9. Optimized structures of supported molybdenum oxide species showing (A) Lewis acidity and (B) Brønsted acidity. The values shown here represent bond distances (Å) in the optimized interaction complexes.

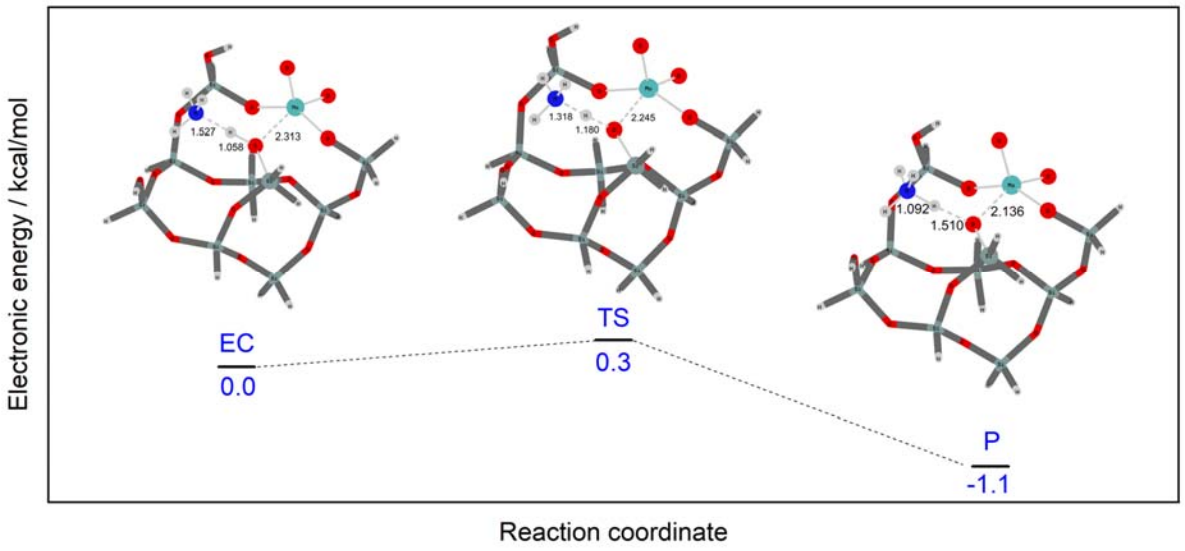

Fig. 10. Reaction energy diagram for the protonation step. The values shown next to bonds in the calculated structures represent bond distances (Å). **EC** stands for encounter complex, **TS** for transition state and **P** for product.

However, the experimental results also revealed that silanol groups are the only possible candidates for the Brønsted acidic sites in presence of molybdenum oxide species. Therefore,

three different structures of di-oxo (Si—O—)$_2$Mo(=O)$_2$ units were generated in the framework of the silsesquioxane cluster ($Si_8O_{12}H_8$) by anchoring the molybdenum atom on top (Fig. S5A) or at the corner (Fig. S5B) of the silsesquioxane cluster, or by connecting the molybdenum oxide unit directly to the silanol group (Fig. S5C). Initially, an ammonia molecule was located closely to the H atom of the silanol group in the generated adsorption complex (distance of H_3N-(HOSi): ~1.0 Å). As criterion of Brønsted acidity the bond distance after geometry optimization should be close to the N-H distance in the ammonium ion (< 1.1 Å). However, in the models applied in Fig. S5, no ammonium ion was formed, because the N-H distance in N---HO-Si remains > 1.6 Å, resembling the energetically favored situation in case of bare SBA-15 (Fig. S4).

As proposed in our previous study [40], increasing the surface density of MoO_x species may induce a modification of the anchoring position of Mo resulting in 'high energy sites' which may be more relevant to catalysis. To acknowledge this, a structure containing a six-membered ring of molybdenum and silicon atoms, as compared to the four or five-membered rings in the models above (Fig. S5), was generated (Fig. 9B) [45]. Such a strained configuration resulted in an N-H distance of 1.09 Å in the energetically optimized adsorption complex, hence, the interaction of the ammonia molecule with the silanol group results in a nitrogen atom that is in contact with four H atoms in a distance < 1.1 Å, similar like in an ammonium ion. As illustrated in Figure 10, the activation barrier for the protonation of ammonia by the silanol group is small (0.3 kcal/mol), which is easy to overcome at room temperature. The transition state structure was confirmed by an intrinsic reaction coordinate (IRC) calculation and frequency calculation (Figure S6). Along the reaction coordinate, the H_3N---H distance gradually decreases resulting in an elongation of O-H bond in the silanol group (Figure S6) and an approach of oxygen in the silanol group towards the molybdenum atom (Fig. 10). Note that due to the close distance of the oxygen atom

in the silanol group to the molybdenum atom in the present model (Fig. 9B), a pseudo-bridging silanol group Si—O(H)---Mo(=O)$_2$ is formed in analogy to the situation in amorphous silica-alumina [63]. The adsorption complex is stabilized by the interaction of the negatively charged oxygen in the "deprotonated" "Si—O$^-$" moiety with the adjacent coordinative unsaturated molybdenum atom (Fig. 11). The present calculation results suggest that the presence of Brønsted acid sites can be an indicator of 'high energy sites' in silica-supported molybdenum oxides catalysts.

4. CONCLUSIONS

The current investigation deals with the origin of Lewis and Brønsted acidity in silica-supported molybdenum oxide catalysts by applying ammonia adsorption. While the bare silica support shows no significant adsorption of ammonia, a linear correlation between the Mo density on the surface of silica-supported molybdenum oxide and the density of adsorbed ammonia molecules was experimentally verified. The quantification of weak acid sites, like in the present case, needs, however, to be handled with care. The surface coverage with ammonia is dependent on the adsorption condition (T, p). Full coverage may not be achieved at all condition applied, in particular not when physically adsorbed ammonia is removed by evacuation or purging with inert gas.

Based on temperature-programmed desorption of ammonia and the analysis of adsorption isotherms of ammonia measured by FTIR spectroscopy we propose that every surface molybdenum atom is involved in the interaction with ammonia, either as Lewis or as Brønsted acid site according to the mechanism presented in Fig. 11.

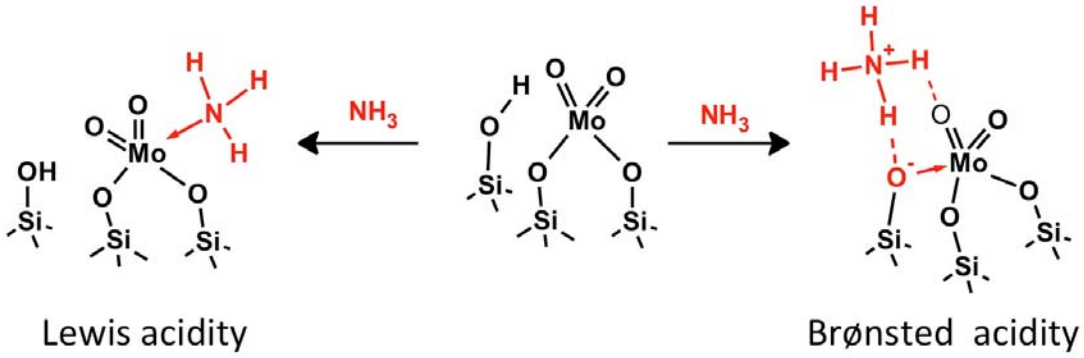

Fig. 11. Proposed origin of Lewis and Brønsted acidity in silica-supported molybdenum oxide monolayer catalysts.

We suggest that Brønsted acid sites are formed due to the interaction between silanol groups and adjacent surface molybdate species. Thus, the present work provides an explanation for the origin of acidity in mixed MoO_3-SiO_2 oxides that is lacking in fundamental understanding so far. The experimental evidence obtained by FTIR and TPD analysis of ammonia adsorption on well-defined model catalysts is supported by model calculations, which allow atomic insight into Lewis acid-base interactions between coordinatively unsaturated Mo atom on the surface and ammonia molecules as well as the protonation of ammonia by acidic silanol groups that are generated due to the presence of MoO_x in the system. The consistent description highlights similarities to the mechanism of acidity generation on the surface of amorphous silica-alumina [15, 63, 66]. The analogy suggests that oxide surface structures, which allow proton transfer from surface OH groups to an adsorbed base, need to fulfill general geometric requirements irrespective of the chemical compositions of the amorphous solid, which calls, however, for further systematic studies to analyze thermodynamic properties and reactivity of a broader variety of complex mixed oxides by combining experimental and theoretical tools.

ACKNOWLEDGMENT

The authors thank Maike Hashagen for her extensive help in experiments and data processing, Prof. Klaus Hermann for fruitful discussions, and the Computer Support Group of the Fritz-Haber-Institut for providing computational resources. K.A. is grateful to Mitsubishi Gas Chemical Co. Inc. for a fellowship.

References

[1] K. Tanabe, W.F. Hölderich, Industrial application of solid acid–base catalysts, Applied Catalysis A: General, 181 (1999) 399-434.
[2] A. Corma, Inorganic Solid Acids and Their Use in Acid-Catalyzed Hydrocarbon Reactions, Chemical Reviews, 95 (1995) 559-614.
[3] S. Yamaguchi, M. Yabushita, M. Kim, J. Hirayama, K. Motokura, A. Fukuoka, K. Nakajima, Catalytic Conversion of Biomass-Derived Carbohydrates to Methyl Lactate by Acid−Base Bifunctional γ-Al2O3, ACS Sustainable Chemistry & Engineering, 6 (2018) 8113-8117.
[4] H. Kobayashi, A. Fukuoka, Synthesis and utilisation of sugar compounds derived from lignocellulosic biomass, Green Chemistry, 15 (2013) 1740-1763.
[5] J. Weitkamp, Catalytic Hydrocracking—Mechanisms and Versatility of the Process, ChemCatChem, 4 (2012) 292-306.
[6] R. Schlögl, Heterogeneous Catalysis, Angewandte Chemie International Edition, 54 (2015) 3465-3520.
[7] E.G. Derouane, J.C. Védrine, R.R. Pinto, P.M. Borges, L. Costa, M.A.N.D.A. Lemos, F. Lemos, F.R. Ribeiro, The Acidity of Zeolites: Concepts, Measurements and Relation to Catalysis: A Review on Experimental and Theoretical Methods for the Study of Zeolite Acidity, Catalysis Reviews, 55 (2013) 454-515.
[8] J.A. Lercher, C. Gründling, G. Eder-Mirth, Infrared studies of the surface acidity of oxides and zeolites using adsorbed probe molecules, Catalysis Today, 27 (1996) 353-376.
[9] I.L.C. Buurmans, B.M. Weckhuysen, Heterogeneities of individual catalyst particles in space and time as monitored by spectroscopy, Nat Chem, 4 (2012) 873-886.
[10] S. Bordiga, C. Lamberti, F. Bonino, A. Travert, F. Thibault-Starzyk, Probing zeolites by vibrational spectroscopies, Chemical Society Reviews, 44 (2015) 7262-7341.
[11] M. Bevilacqua, T. Montanari, E. Finocchio, G. Busca, Are the active sites of protonic zeolites generated by the cavities?, Catalysis Today, 116 (2006) 132-142.
[12] V. Van Speybroeck, K. Hemelsoet, L. Joos, M. Waroquier, R.G. Bell, C.R.A. Catlow, Advances in theory and their application within the field of zeolite chemistry, Chemical Society Reviews, 44 (2015) 7044-7111.
[13] R.A. van Santen, Quantum-chemistry of zeolite acidity, Catalysis Today, 38 (1997) 377-390.

[14] S. Shaikhutdinov, H.-J. Freund, Metal-Supported Aluminosilicate Ultrathin Films as a Versatile Tool for Studying the Surface Chemistry of Zeolites, ChemPhysChem, 14 (2013) 71-77.
[15] F. Leydier, C. Chizallet, A. Chaumonnot, M. Digne, E. Soyer, A.-A. Quoineaud, D. Costa, P. Raybaud, Brønsted acidity of amorphous silica–alumina: The molecular rules of proton transfer, Journal of Catalysis, 284 (2011) 215-229.
[16] K. Arata, Preparation of superacids by metal oxides for reactions of butanes and pentanes, Applied Catalysis A: General, 146 (1996) 3-32.
[17] G. Busca, The surface acidity of solid oxides and its characterization by IR spectroscopic methods. An attempt at systematization, Physical Chemistry Chemical Physics, 1 (1999) 723-736.
[18] M.A. Banares, H.C. Hu, I.E. Wachs, Molybdena on Silica Catalysts: Role of Preparation Methods on the Structure-Selectivity Properties for the Oxidation of Methanol, Journal of Catalysis, 150 (1994) 407-420.
[19] S.T. Oyama, W. Zhang, True and Spectator Intermediates in Catalysis: The Case of Ethanol Oxidation on Molybdenum Oxide As Observed by in Situ Laser Raman Spectroscopy, Journal of the American Chemical Society, 118 (1996) 7173-7177.
[20] T.K. Shokhireva, T.M. Yurieva, N.N. Chumachenko, Catalytic properties of silica-molybdenum catalysts in propylene oxidation, Reaction Kinetics and Catalysis Letters, 14 77-80.
[21] T.-C. Liu, M. Forissier, G. Coudurier, J.C. Vedrine, Properties of molybdate species supported on silica, Journal of the Chemical Society, Faraday Transactions 1: Physical Chemistry in Condensed Phases, 85 (1989) 1607-1618.
[22] N. Ohler, A.T. Bell, Selective oxidation of methane over MoOx/SiO2: isolation of the kinetics of reactions occurring in the gas phase and on the surfaces of SiO2 and MoOx, Journal of Catalysis, 231 (2005) 115-130.
[23] Y. Lou, H. Wang, Q. Zhang, Y. Wang, SBA-15-supported molybdenum oxides as efficient catalysts for selective oxidation of ethane to formaldehyde and acetaldehyde by oxygen, Journal of Catalysis, 247 (2007) 245-255.
[24] J. Handzlik, J. Ogonowski, J. Stoch, M. Mikołajczyk, P. Michorczyk, Properties and metathesis activity of molybdena-alumina, molybdena-silica-alumina and molybdena-silica catalysts—a comparative study, Applied Catalysis A: General, 312 (2006) 213-219.
[25] K. Amakawa, J. Kröhnert, S. Wrabetz, B. Frank, F. Hemmann, C. Jäger, R. Schlögl, A. Trunschke, Active Sites in Olefin Metathesis over Supported Molybdena Catalysts, ChemCatChem, 7 (2015) 4059-4065.
[26] K. Amakawa, S. Wrabetz, J. Kröhnert, G. Tzolova-Müller, R. Schlögl, A. Trunschke, In Situ Generation of Active Sites in Olefin Metathesis, Journal of the American Chemical Society, 134 (2012) 11462-11473.
[27] S. Bednárová, B. Wichterlová, P. Jíru, Influence of Mo ions and OH groups on l-butene isomerization, Reaction Kinetics and Catalysis Letters, 25 (1984) 59-63.
[28] F. Janowski, A. Sofianos, F. Wolf, The role of acidity of MoO3−SiO2 and WO3−SiO2 catalysts, Reaction Kinetics and Catalysis Letters, 12 (1979) 157-163.
[29] E. Alsdorf, W. Hanke, K.H. Schnabel, E. Schreier, Infrared studies on the interaction of ammonia and water on MoO3SiO2 catalysts, Journal of Catalysis, 98 (1986) 82-87.

[30] M.A. Banares, H.C. Hu, I.E. Wachs, Genesis and Stability of Silicomolybdic Acid on Silica-Supported Molybdenum Oxide Catalysts: In-Situ Structural-Selectivity Study on Selective Oxidation Reactions, Journal of Catalysis, 155 (1995) 249-255.
[31] N.C. Ramani, D.L. Sullivan, J.G. Ekerdt, Isomerization of 1-Butene over Silica-Supported Mo(VI), W(VI), and Cr(VI), Journal of Catalysis, 173 (1998) 105-114.
[32] T.V. Kotbagi, A.V. Biradar, S.B. Umbarkar, M.K. Dongare, Isolation, Characterization, and Identification of Catalytically Active Species in the MoO3/SiO2 Catalyst during Solid Acid Catalyzed Reactions, ChemCatChem, 5 (2013) 1531-1537.
[33] D. Teschner, E.M. Vass, R. Schlögl, Photoelectron Spectroscopy of Catalytic Oxide Materials, in: S.D. Jackson, J.S.J. Hargreaves (Eds.) Metal Oxide Catalysis, Wiley-VCH: Weinheim, 2009, pp. 243-298.
[34] S. Ramani, J.F. Richardson, R. Miranda, Molecular modelling study of solid acidity in molybdenum oxide supported on silica-alumina, Modelling and Simulation in Materials Science and Engineering, 7 (1999) 459.
[35] J.C. Védrine, Acid–base characterization of heterogeneous catalysts: an up-to-date overview, Research on Chemical Intermediates, 41 (2015) 9387-9423.
[36] A.A. Davydov, Molecular spectroscopy of oxide catalyst surfaces, John Wiley & Sons Ltd., Chinchester, 2003.
[37] C.-M. Wang, R.Y. Brogaard, B.M. Weckhuysen, J.K. Nørskov, F. Studt, Reactivity Descriptor in Solid Acid Catalysis: Predicting Turnover Frequencies for Propene Methylation in Zeotypes, The Journal of Physical Chemistry Letters, 5 (2014) 1516-1521.
[38] E.H. Teunissen, F.B. Van Duijneveldt, R.A. Van Santen, Interaction of ammonia with a zeolitic proton: ab initio quantum-chemical cluster calculations, The Journal of Physical Chemistry, 96 (1992) 366-371.
[39] E.H. Teunissen, R.A. Van Santen, A.P.J. Jansen, F.B. Van Duijneveldt, Ammonium in zeolites: coordination and solvation effects, The Journal of Physical Chemistry, 97 (1993) 203-210.
[40] K. Amakawa, L. Sun, C. Guo, M. Hävecker, P. Kube, I.E. Wachs, S. Lwin, A.I. Frenkel, A. Patlolla, K. Hermann, R. Schlögl, A. Trunschke, How Strain Affects the Reactivity of Surface Metal Oxide Catalysts, Angewandte Chemie International Edition, 52 (2013) 13553-13557.
[41] V.A. Matyshak, O.V. Krylov, Problems of Quantitative Spectroscopic Measurements in Heterogeneous Catalysis: Molar Absorption Coefficients of Vibrations in Adsorbed Substances, Kinetics and Catalysis, 43 (2002) 391-407.
[42] C.S. Guo, K. Hermann, M. Hävecker, J.P. Thielemann, P. Kube, L.J. Gregoriades, A. Trunschke, J. Sauer, R. Schlögl, Structural Analysis of Silica-Supported Molybdena Based on X-ray Spectroscopy: Quantum Theory and Experiment, The Journal of Physical Chemistry C, 115 (2011) 15449-15458.
[43] C.S. Guo, K. Hermann, M. Hävecker, A. Trunschke, R. Schlögl, Silica-Supported Titania Species: Structural Analysis from Quantum Theory and X-ray Spectroscopy, The Journal of Physical Chemistry C, 116 (2012) 22449-22457.
[44] S. Klokishner, O. Reu, G. Tzolova-Müller, R. Schlögl, A. Trunschke, Apparent Absorption Spectra of Silica Supported Vanadium–Titanium Oxide Catalysts: Experimental Study and Modeling, The Journal of Physical Chemistry C, 118 (2014) 14677-14691.
[45] J. Handzlik, J. Ogonowski, Structure of Isolated Molybdenum(VI) and Molybdenum(IV) Oxide Species on Silica: Periodic and Cluster DFT Studies, The Journal of Physical Chemistry C, 116 (2012) 5571-5584.

[46] D. Maganas, A. Trunschke, R. Schlögl, F. Neese, A unified view on heterogeneous and homogeneous catalysts through a combination of spectroscopy and quantum chemistry, Faraday Discussions, 188 (2016) 181-197.
[47] F. Weigend, R. Ahlrichs, Balanced basis sets of split valence, triple zeta valence and quadruple zeta valence quality for H to Rn: Design and assessment of accuracy, Physical Chemistry Chemical Physics, 7 (2005) 3297-3305.
[48] F. Weigend, Accurate Coulomb-fitting basis sets for H to Rn, Physical Chemistry Chemical Physics, 8 (2006) 1057-1065.
[49] S. Grimme, S. Ehrlich, L. Goerigk, Effect of the damping function in dispersion corrected density functional theory, Journal of Computational Chemistry, 32 (2011) 1456-1465.
[50] M.J. Frisch, G.W. Trucks, H.B. Schlegel, G.E. Scuseria, M.A. Robb, J.R. Cheeseman, G. Scalmani, V. Barone, B. Mennucci, G.A. Petersson, H. Nakatsuji, M. Caricato, X. Li, H.P. Hratchian, A.F. Izmaylov, J. Bloino, G. Zheng, J.L. Sonnenberg, M. Hada, M. Ehara, K. Toyota, R. Fukuda, J. Hasegawa, M. Ishida, T. Nakajima, Y. Honda, O. Kitao, H. Nakai, T. Vreven, J.A. Montgomery, J.E. Peralta, F. Ogliaro, M. Bearpark, J.J. Heyd, E. Brothers, K.N. Kudin, V.N. Staroverov, R. Kobayashi, J. Normand, K. Raghavachari, A. Rendell, J.C. Burant, S.S. Iyengar, J. Tomasi, M. Cossi, N. Rega, J.M. Millam, M. Klene, J.E. Knox, J.B. Cross, V. Bakken, C. Adamo, J. Jaramillo, R. Gomperts, R.E. Stratmann, O. Yazyev, A.J. Austin, R. Cammi, C. Pomelli, J.W. Ochterski, R.L. Martin, K. Morokuma, V.G. Zakrzewski, G.A. Voth, P. Salvador, J.J. Dannenberg, S. Dapprich, A.D. Daniels, Farkas, J.B. Foresman, J.V. Ortiz, J. Cioslowski, D.J. Fox, Gaussian 09, Revision D.01, in, Wallingford CT, 2009.
[51] E.L. Lee, I.E. Wachs, In Situ Spectroscopic Investigation of the Molecular and Electronic Structures of SiO2 Supported Surface Metal Oxides, The Journal of Physical Chemistry C, 111 (2007) 14410-14425.
[52] G. Mestl, T.K.K. Srinivasan, Raman spectroscopy of monolayer-type catalysts: Supported molybdenum oxides, Catalysis Reviews-Science and Engineering, 40 (1998) 451-570.
[53] J.P. Baltrus, L.E. Makovsky, J.M. Stencel, D.M. Hercules, Quantitative Raman spectrometric determination of molybdenum trioxide and tungsten trioxide in supported catalysts, Analytical Chemistry, 57 (1985) 2500-2503.
[54] N. Kakuta, K. Tohji, Y. Udagawa, Molybdenum oxide structure on silica-supported catalysts studied by Raman spectroscopy and EXAFS, The Journal of Physical Chemistry, 92 (1988) 2583-2587.
[55] E.L. Lee, I.E. Wachs, In Situ Raman Spectroscopy of SiO2-Supported Transition Metal Oxide Catalysts: An Isotopic 18O-16O Exchange Study, The Journal of Physical Chemistry C, 112 (2008) 6487-6498.
[56] M. Niwa, N. Katada, M. Sawa, Y. Murakami, Temperature-Programmed Desorption of Ammonia with Readsorption Based on the Derived Theoretical Equation, The Journal of Physical Chemistry, 99 (1995) 8812-8816.
[57] C.E. Webster, R.S. Drago, M.C. Zerner, Molecular Dimensions for Adsorptives, Journal of the American Chemical Society, 120 (1998) 5509-5516.
[58] B. Civalleri, P. Ugliengo, First Principles Calculations of the Adsorption of NH3 on a Periodic Model of the Silica Surface, The Journal of Physical Chemistry B, 104 (2000) 9491-9499.
[59] I. Langmuir, THE CONSTITUTION AND FUNDAMENTAL PROPERTIES OF SOLIDS AND LIQUIDS. PART I. SOLIDS, Journal of the American Chemical Society, 38 (1916) 2221-2295.

[60] N. Cardona Martínez, J.A. Dumesic, Thermochemical Characterization, in: Handbook of Heterogeneous Catalysis, Wiley-VCH Verlag GmbH & Co. KGaA, 2008.
[61] N. Katada, M. Niwa, Analysis of Acidic Properties of Zeolitic and Non-Zeolitic Solid Acid Catalysts Using Temperature-Programmed Desorption of Ammonia, Catal Surv Asia, 8 161-170.
[62] A. Auroux, A. Gervasini, Microcalorimetric study of the acidity and basicity of metal oxide surfaces, The Journal of Physical Chemistry, 94 (1990) 6371-6379.
[63] C. Chizallet, P. Raybaud, Acidity of Amorphous Silica–Alumina: From Coordination Promotion of Lewis Sites to Proton Transfer, Chemphyschem, 11 (2010) 105-108.
[64] N. Katada, K. Nouno, J.K. Lee, J. Shin, S.B. Hong, M. Niwa, Acidic Properties of Cage-Based, Small-Pore Zeolites with Different Framework Topologies and Their Silicoaluminophosphate Analogues, The Journal of Physical Chemistry C, 115 (2011) 22505-22513.
[65] A. Trunschke, B. Hunger, Characterization of Acidic OH Groups in Y-Type Zeolites by Means of Different Methods of Temperature-Programmed Desorption (TPD) of Ammonia, Topics in Catalysis, 19 (2002) 215-223.
[66] M. Valla, A.J. Rossini, M. Caillot, C. Chizallet, P. Raybaud, M. Digne, A. Chaumonnot, A. Lesage, L. Emsley, J.A. van Bokhoven, C. Copéret, Atomic Description of the Interface between Silica and Alumina in Aluminosilicates through Dynamic Nuclear Polarization Surface-Enhanced NMR Spectroscopy and First-Principles Calculations, Journal of the American Chemical Society, 137 (2015) 10710-10719.